

K. TAKAHASHI^{1,2}
Y. WANG¹
K. LEE^{1,3}
G. CAO^{1,✉}

Fabrication and Li⁺-intercalation properties of V₂O₅-TiO₂ composite nanorod arrays

¹ Materials Science and Engineering, University of Washington, Seattle WA, USA
² Steel Research Laboratory, JFE Steel Corporation, Tokyo, Japan
³ Materials Engineering, Soonchunhyang University, Chungnam, Korea

Received: 18 July 2005 / Accepted: 28 July 2005
Published online: 30 September 2005 • © Springer-Verlag 2005

ABSTRACT A capillary-enforced template-based method has been applied to fabricate V₂O₅-TiO₂ composite nanorod arrays via filling mixture of VOSO₄ and TiOSO₄ solutions into the pores of polycarbonate membrane. For comparison purposes, pure V₂O₅ nanorod arrays were prepared through the similar template-based method with V₂O₅ sol and the sol was synthesized through the V₂O₅-H₂O₂ route. The nanorods covered completely a large area and projected from the surface of ITO substrate. The addition of TiO₂ to V₂O₅ has demonstrated to greatly affect the Li⁺ intercalation capacity of V₂O₅. For example, V₂O₅-TiO₂ nanorod array with molar ratio V/Ti = 75/25 delivered 1.5 times discharge capacity of V₂O₅ nanorods at a current density of 92 mA/g. Such improvement in the intercalation properties was ascribed to the change of crystallinity and possible modification in lattice structure and interaction forces between adjacent layers in V₂O₅.

PACS 81.05.Je; 82.45.Yz; 81.10.Dn; 81.20.Fw; 82.47.Aa

1 Introduction

Vanadium pentoxide (V₂O₅) has attracted a lot of attention for its electrochemical applications, such as pseudocapacitor [1–3], electrochromic coatings [4, 5] and actuators [6]. V₂O₅ has a layered structure and has the ability to intercalate cations between the adjacent layers [7, 8]. This intercalation process is accompanied with a change of dimension, due to the expansion or contraction of the distance between adjacent layers, and a change of color, due to the change of valence states of vanadium ions. When V₂O₅ intercalates Li⁺, electrical energy is stored in the form of chemical potential. Energy is released from the intercalated V₂O₅ in the form of electricity, when Li⁺ diffuses out [9]. For electrochemical pseudocapacitor applications, the charge/discharge rate and energy storage capacity are important parameters.

A large surface area is desired to achieve large storage capacity since only a surface layer is practically used for the intercalation of ions, and a short diffusion distance favors fast charge and discharge process. Usually fine powders are used for achieving high energy storage capacity [10]. For example, it has been demonstrated that single crystal V₂O₅ nanorod arrays have approximately five times higher applicable current density than the sol-gel derived film, and in a given current density, nanorod-array electrode can intercalate up to five times higher amount of lithium ions [11, 12].

Another approach to increase the intercalation capacity of V₂O₅ is to modify its crystalline structure and the interaction force between the adjacent layers. When the distance between the adjacent layers of V₂O₅ increases, the insertion capacity increases. For example, hydrated vanadium pen-

toxide, V₂O₅·*n*H₂O, possesses the Li intercalation capacity about 1.4 times larger than that of V₂O₅ [13]. The distance between the adjacent layers in V₂O₅·*n*H₂O is 11.52 Å [14], as compared with a distance between layers of 4.56 Å in orthorhombic V₂O₅. Doping or substitution in V₂O₅ by other cations with different valence states have been used to tailor the interaction forces between two adjacent layers in the intercalation compound. Several materials, such as Ni [15], Ce [16], Ag and Cu [17], have been reported to enhance the capacity of V₂O₅ by forming bronze structures with it. Titanium has the valence state +4 in TiO₂ and the diameter of titanium is similar to that of vanadium with a coordination number of 6. Özer et al. have prepared titanium-doped vanadium pentoxide, (100 - *x*)V₂O₅-*x*TiO₂ (*x* < 20) films by using sol-gel dip coating techniques; the CV curve of V₂O₅-TiO₂ composite films fired at 300 °C exhibited a significant change compared to that of pure V₂O₅ [18]. This suggests that doping with Ti can change the electrochemical properties of V₂O₅; however, these films sintered at 300 °C were amorphous and their electrochemical performance was less sustainable than crystalline V₂O₅. Most recently, Lee and Cao have found that the electrochemical intercalation properties of V₂O₅ have been significantly enhanced with the addition of TiO₂ [19]. It is also well known in the literature that the presence of TiO₂ appreciably improves the cyclic fatigue resistance of V₂O₅ [20].

To improve electrochemical properties of V₂O₅, we have combined both approaches mentioned above, i.e., modifying microstructure and chemical

✉ Fax: 01-206-543-3100, E-mail: gzcao@u.washington.edu

composition, and synthesized nanorods of V_2O_5 - TiO_2 composites. Arrays of V_2O_5 - TiO_2 nanorods were prepared by filling the mixture of $VOSO_4$ and $TiOSO_4$ solutions into polycarbonate (PC) membranes via capillary forces. For comparison purposes, nanorod arrays of pure V_2O_5 were prepared by filling $V_2O_5 \cdot nH_2O$ sol into the PC membranes via capillary forces as well. Li^+ -intercalation properties of these V_2O_5 - TiO_2 composite nanorod arrays and pure V_2O_5 nanorod arrays have been investigated and discussed.

2 Experiments

A VO^{2+} solution was prepared by dissolving $VOSO_4$ (Alfa Aesar) into de-ionized H_2O and H_2SO_4 in a molar concentration of 0.1 M; the resulting solution has a blue color and a pH of 1.8. A TiO^{2+} solution was prepared by diluting $TiOSO_4$ solution (15 wt. % in diluted H_2SO_4 , Aldrich) with de-ionized H_2O to a concentration of 0.1 M; its pH value was adjusted to 1.8 by adding NH_4OH . VO^{2+} and TiO^{2+} solutions were then aged for a week in air and admixed with molar ratios of 75/25 and 50/50. $V_2O_5 \cdot nH_2O$ sols were synthesized based on a method reported by Fontenot et al. with V_2O_5 (Alfa Aesar) and 30% H_2O_2 (J.T. Baker) as precursors [21]. 0.136 g V_2O_5 powder was dissolved in 2 ml de-ionized H_2O and 0.603 ml H_2O_2 solution. The suspension was stirred until V_2O_5 powder totally dissolved, resulting in a clear and dark red solution. The solution was then sonicated to get a yellow-brown gel which was dispersed into de-ionized H_2O in a molar concentration of 0.025 M. The primary vanadium species in the colloidal dispersion are nanoparticles of hydrated vanadium oxide.

V_2O_5 - TiO_2 composite nanorod arrays were grown in PC templates by means of capillary force induced filling. The templates used were radiation track-etched hydrophilic PC membrane (Millipore, Bedford, MA) with pore diameters of 400 nm and thickness of 10 μm . An excessive amount of the precursor solution was dropped onto ITO substrates, and a PC membrane was placed on the top of the solution at ambient pressure and room temperature for 4 h to allow complete filling and solidi-

fication of solution. The filled template on ITO substrate was then dried at 70 $^{\circ}C$ for 8 h in air and fired at 485 $^{\circ}C$ for 1 h to remove the PC membranes through pyrolysis and oxidation as well as to densify the nanorod arrays. Pure V_2O_5 nanorod arrays were obtained by filling $V_2O_5 \cdot nH_2O$ sol into 400-nm-diameter pores of the PC membranes through the similar process. The filled template on ITO substrate was dried at 110 $^{\circ}C$ for 8 h in air before staying under ambient conditions for 4 h. The sample was then fired at 485 $^{\circ}C$ for 1 h to remove PC membranes. All the samples prepared have similar geometric area, similar thickness and similar mass of material.

V_2O_5 - TiO_2 nanorod arrays were characterized by means of scanning electron microscopy (SEM, JEOL JSM-5200), and X-ray diffractometry (XRD, Philips PW1820). Electrochemical properties of V_2O_5 - TiO_2 nanorod arrays were investigated using a standard three-electrode cell. A 1 M- $LiClO_4$ solution in propylene carbonate was used as the electrolyte, and a Pt mesh was used as the counter electrode with $Ag/AgNO_3$ as the reference electrode. Cyclic voltammetry and chronopotentiometric measurements were carried out by potentiostat/galvanostat (Model 605B, CH Instruments).

3 Results and Discussion

Figure 1 shows typical SEM images of (a) pure V_2O_5 nanorod arrays (b) V_2O_5 - TiO_2 composite nanorods (molar ratio V/Ti = 50/50) grown in 400 nm PC membranes and fired at 485 $^{\circ}C$ for 1 h in air. These nanorods project from the surface of ITO substrate like bristles of a brush and the V_2O_5 - TiO_2 composite nanorods are less smooth than pure V_2O_5 nanorods. V_2O_5 - TiO_2 nanorods (molar ratio V/Ti = 75/25) have similar morphology to composite nanorods with molar ratio V/Ti = 50/50; therefore, its SEM is not shown here. Figure 2 present schematics that illustrate the fabrication procedure of the nanorod arrays. The V_2O_5 - TiO_2 nanorods were grown by solution filling into PC template pores with capillary force. The solution was drawn up into and filled up the pores of PC membrane; air in the pores and the vapor from the solution were evaporated

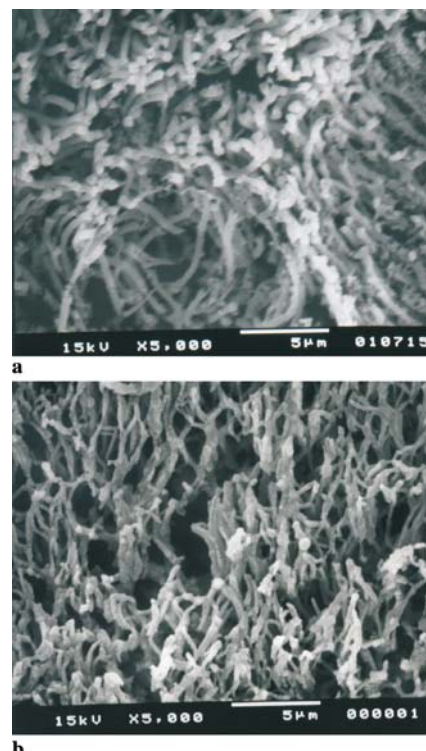


FIGURE 1 SEM images of (a) pure V_2O_5 nanorods grown in PC membranes with 400-nm-diameter pores using capillary force method and fired at 485 $^{\circ}C$ and (b) V_2O_5 - TiO_2 (molar ratio V/Ti = 50/50) composite nanorod arrays

from the top surface of the PC template. As the solvent evaporated from the surface and the concentration enriched at the top of the pores, precipitation or gelation occurred first at the top of the pores and subsequently proceeded throughout the entire pores. However, our early experiments show that no nanorods could grow by filling fresh solutions. Aging of solutions in ambient environment played a critical role. Obviously, in order to grow nanorod arrays, the solution filled in the pores must be converted to a solid phase. During aging at ambient environment, both $TiOSO_4$ and $VOSO_4$ solutions were found to increase their solid concentrations and pH values due to the evaporation of solvent and acids, and went through partial hydrolysis and condensation processes. Capillary force induced filling of solution or colloidal dispersion in templates has demonstrated to be an efficiency approach for the synthesis of composite nanorod arrays. Although many elegant techniques have been developed for the synthesis of nanorod arrays [22], many of them can not be used for growing composite nanorod arrays. For example,

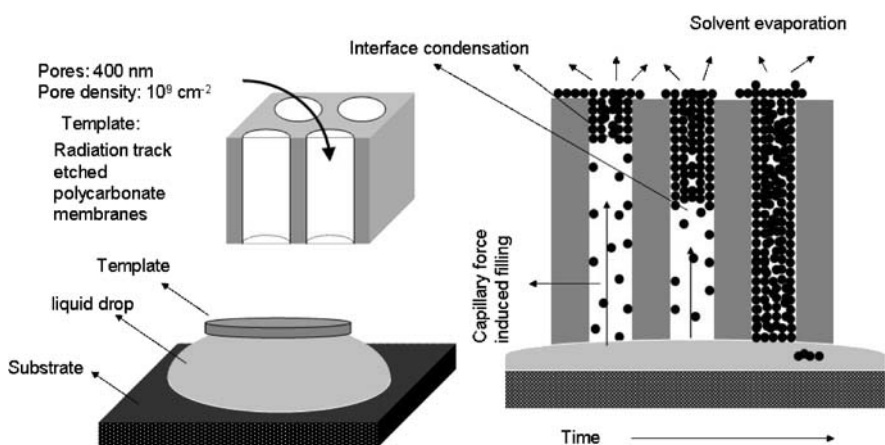


FIGURE 2 Schematics of fabrication process of V_2O_5 - TiO_2 nanorod arrays or V_2O_5 nanorod arrays. *Top picture on the left*: three-dimensional view of a polycarbonate membrane; *bottom picture on the left*: set-up for fabrication of nanorod arrays; *schematic on the right*: growth process of nanorod arrays

sol electrophoretic deposition [23] can be used to prepare single-phase nanorod arrays; otherwise, if an electrical field is applied on multiple-phase sols, different sol particles have different surface charges and phase segregation will occur so that homogeneous composition of the product can not be obtained. Centrifugation force has been used to grow nanorod arrays as well [24]. However, for multiple-phase systems, the size and shape of different sol particles may differ; thus, phase segregation may occur, which will prevent the formation of homogeneous nanocomposite nanorods as well. Solvent-evaporation induced deposition provides a simple and elegant method for preparing composite nanorod arrays. Its mechanism is similar to that of slip-casting [25]. The nanorods in the present work were synthesized from solutions that consist of both Ti and V ions homogeneously mixed. Aging has demonstrated to be a critical step required for the formation of the desired composite nanorods. During the aging process, moisture from the ambient is expected to be up-taken by solution and partial hydrolysis and condensation process is anticipated to proceed resulting in the formation of nanoclusters.

Figure 3 shows XRD patterns of the V_2O_5 - TiO_2 nanorod arrays attached onto ITO substrate after firing. The XRD patterns clearly demonstrated that crystalline V_2O_5 phase and TiO_2 anatase phase coexist. In this research, VOSO_4 (valence state of V is +4) was used as the precursor material for preparing the V_2O_5 - TiO_2 composite nanorod array.

Although VO_2 can form a solid solution with TiO_2 , XRD patterns indicate that no solid solutions were formed in this study. The nanorods studied are basically a mixture of vanadium pentoxide and anatase phase, suggesting V(+4) has been oxidized to V(+5) during the

processing. Careful comparison of XRD patterns suggests that crystallinity of both TiO_2 and V_2O_5 phases deteriorated when the other phase was present. Figure 4 shows the peak heights of (001) of vanadium pentoxide and (101) of anatase as functions of V/Ti molar ratios with ITO as a reference. This figure clearly indicates that mixtures of V/Ti around 50/50 to 75/25 have lower peak heights than that predicted by the simple mixing rule. Crystallization being hindered in the mixed-oxide system is a known phenomenon caused by an increased requirement for diffusion for the crystallization processes to occur in the mixed system. In our separate study, it was found that the presence of other phase indeed results in an appreciable reduction of grain sizes and a change of morphologies of both V_2O_5 and TiO_2 phases [19].

Figure 5a shows cyclic voltammograms of V_2O_5 - TiO_2 nanorod arrays with various V/Ti molar ratios. A scan rate of 10 mV/s was used, in order to

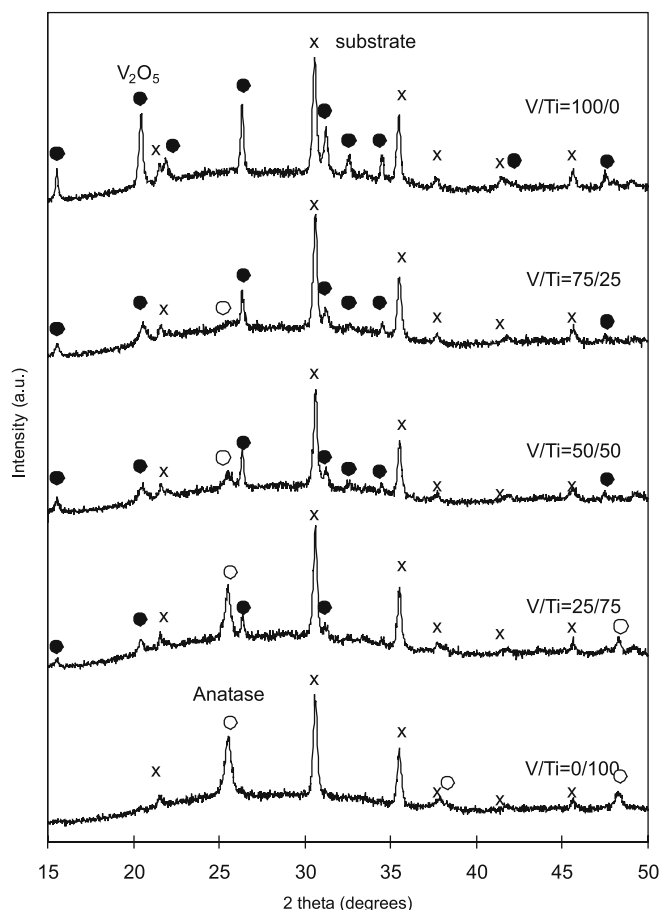


FIGURE 3 X-ray diffraction patterns of the V_2O_5 - TiO_2 nanorods grown onto ITO substrate by capillary force method

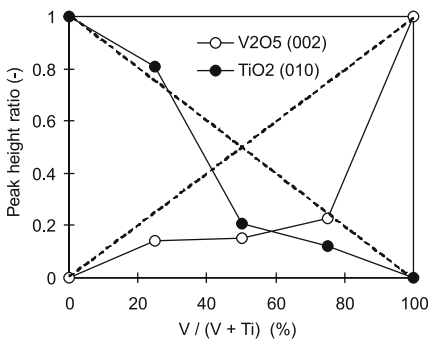


FIGURE 4 The relationship between molar fraction $V/(V+Ti)$ and peak heights of (001) of orthorhombic V_2O_5 and (101) of anatase TiO_2 in XRD spectrums

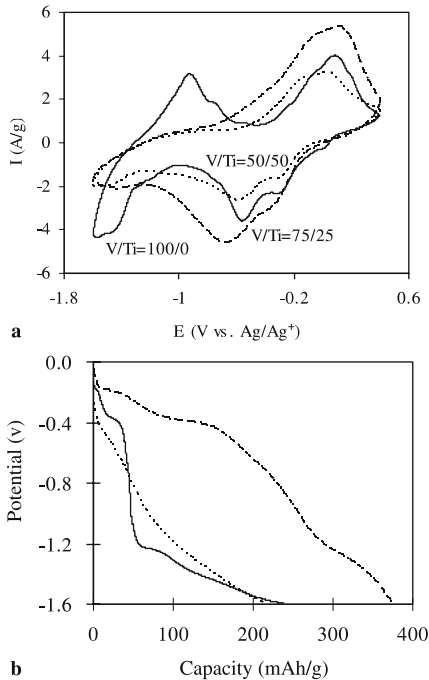


FIGURE 5 (a) Cyclic voltammograms of V_2O_5 - TiO_2 nanorod arrays using a scan rate of 10 mV/sec. (b) Chronopotentiograms of V_2O_5 - TiO_2 nanorod arrays with V/Ti ratios of 100/0, 75/25 and 50/50 at a current density of 92 mA/g. (solid line: $V/Ti = 100/0$; dashed line: $V/Ti = 75/25$; dotted line: $V/Ti = 50/50$)

be consistent to our separate publication on V_2O_5 - TiO_2 composite film [19] and the reported literature on Ti-V-O system [18]. Pure V_2O_5 shows cathodic peaks at -0.3 V, -0.6 V, and -1.5 V, which correspond to Li^+ intercalation, and anodic oxidation peaks at -0.9 V, 0.0 V, and 0.1 V, which are attributed to Li^+ extraction. Along with Ti deposition, peaks shift to lower potential and are more broadened, (two distinct peaks of V_2O_5 at -1.5 V and -0.9 V disappear in the case of V_2O_5 - TiO_2 nanorods), possibly due to the reduction of crystallinity. Figure 5b compares the

chronopotentiograms (CPs) of V_2O_5 - TiO_2 nanorod arrays with V/Ti molar ratios of 100/0, 75/25 and 50/50, at current density of 92 A/g. The CP curve of pure V_2O_5 nanorod array shows a distinct step-wise shape due to its good crystallinity, while the CP curves of V_2O_5 - TiO_2 composite nanorod arrays are less step-wise due to the deteriorated crystallinity as indicated in XRD patterns. For the nanorod array with molar ratio $V/Ti = 50/50$, the CP curve has an almost sloping shape, characteristic of its low-crystalline nature. It is also very clear that the nanorod arrays with molar ratio $V/Ti = 75/25$ have a larger capacity (~ 180 mAh/g) than that of pure V_2O_5 nanorods (~ 120 mAh/g). It is interesting to note that the capacity obtained by CP measurements in Fig. 5b is not proportional to the area of the corresponding CV curve in Fig. 5a. The reason is discussed as follows. The purpose of the CV measurement in Fig. 5a is to find out the potential window for Li-ion intercalation/deintercalation processes. The scan rate, 10 mV/s used in Fig. 5a is the one often referred in the literature and is not calculated from the discharge rate in Fig. 5b. Therefore, discharge rates in Fig. 5a and b are different, and there is no direct correlation in capacities in Fig. 5a and b. The CV of the cathode materials for Li-ion battery is resulted from the reaction between the electrolyte and the confined depth from the surface of the electrode and this confined depth is varied with electrode material. On the other hand, the CP curve is resulted from the fact that how the Li ions are diffused from the surface to inner part of electrode. If the electrode materials have almost same Li diffusion rate, the area of the CV should be n times larger for the material exhibits n times higher capacity. However, if the materials have different Li diffusion rate, the CV and CP does not show the proportional relationship. The addition of TiO_2 to V_2O_5 has diminished the crystallinity of V_2O_5 as shown in XRD patterns in Fig. 3. Furthermore, SEM images in Fig. 1 show the V_2O_5 nanorods are smooth, while the V_2O_5/TiO_2 composite nanorods are less smooth and have granular shape possibly due to the increased requirement for diffusion for the crystallization processes to occur in the mixed oxide system. The change of crystallinity and

morphology may subsequently affect the diffusion rate of Li ions in V_2O_5 for pure V_2O_5 system and V_2O_5/TiO_2 system. It should also be noted that the capacity of nanostructured electrode is less dependent on discharge rate than that of film electrode is. However, the nanorod arrays grown in the 400-nm-dia pores of PC templates in the present work do not bring up all the advantage of large surface area and short diffusion distance of nanostructures due to the large diameter of these nanorods. As a result, the capacities of these nanorod arrays are affected by current densities as shown in Fig. 6.

Figure 6a summarizes and compares the Li^+ intercalation capacity as a function of current density of nanorod arrays with three V/Ti molar ratios. Li^+ intercalation capacity of V_2O_5 - TiO_2 nanorod array is higher than pure V_2O_5 in case of molar ratio $V/Ti = 75/25$, but lower for molar ratio $V/Ti = 50/50$. Figure 6b illustrates the changes in discharge capacity with different molar fraction $V/(V+Ti)$ at a given current density. It is clear that nanorod arrays

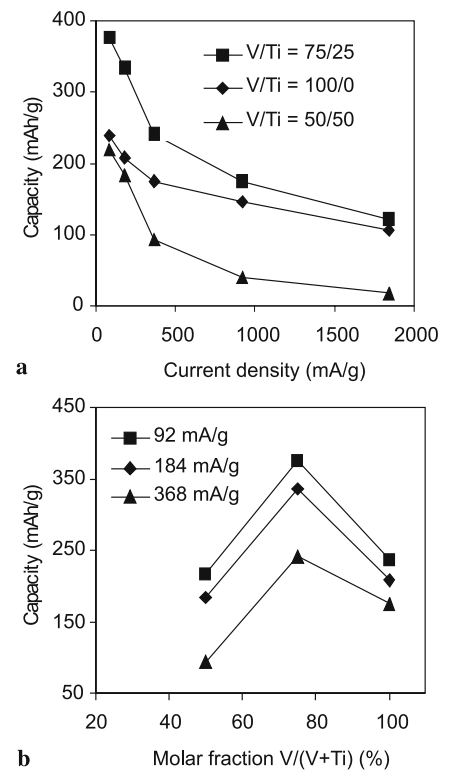


FIGURE 6 (a) Li^+ intercalation capacity vs. current density for V_2O_5 - TiO_2 nanorods with various V/Ti molar ratio, and (b) Li^+ intercalation capacity vs. molar fraction of vanadium at various current densities

with a V/Ti molar ratio of 75/25 have the highest energy storage capacity at all current densities. Such result is similar to Lee and Cao's work on V₂O₅-TiO₂ composite films presented elsewhere [19].

The possible mechanisms for the enhancement of electrochemical intercalation properties may be attributed to the reduced grain size and poor crystallinity. Smaller grains possess a large surface area for intercalation surface reaction and a short diffusion distance for Li ions. The poor crystallinity or partial amorphous may also favor enhanced intercalation due to their more open structure [26]. Although it is known that TiO₂ and V₂O₅ do not form a solid solution, it might be possible that a trace amount of Ti was incorporated into vanadium oxide structure in the present study. The homogeneous solution mixture at the atomic level makes it possible to achieve partial substitution at the V site by a Ti ion during firing. Surca et al. [27] mentioned the possibility of the substitution of V by Ti in amorphous state V₂O₅. The valence state of the Ti ion is smaller than V ion in V₂O₅ and the ionic radius of tetravalent titanium is greater than that of pentavalent vanadium, thus the size and shape of polyhedron may change, which may result in distortion of the pyramidal chain array of VO₅ and render more open space for Li⁺ insertion. The possibility of a trace amount of Ti entering the crystal structure of V₂O₅ can lead to an enlarged distance and weakened interaction force between the adjacent layers so that permits more intercalation of Li ions. However, from XRD patterns in Fig. 3, there is little peak shift for various ratio V/Ti, indicating such replacement of V by Ti is rather small.

It should also be noted that the absolute intercalation capacities of the

pure V₂O₅ and V₂O₅-TiO₂ composite nanorod arrays are smaller than that of single crystal vanadium pentoxide nanorod arrays reported previously [8]. In addition, the intercalation behavior of both pure V₂O₅ and V₂O₅-TiO₂ composite nanorod arrays is a little different from that of pure V₂O₅ and V₂O₅-TiO₂ films that was reported earlier [19]. These differences may well be contributed to the different synthesis and processing methods applied in the study. It is well known that the electrochemical intercalation properties are sensitively dependent on the processing methods and conditions [28].

4 Conclusions

V₂O₅-TiO₂ composite nanorod arrays were grown by the capillary-enforced template-based method from solution. These nanorods covered completely a large area and projected from the surface of ITO substrate. The crystalline conditions of these mixed nanorods were poor, indicating that Ti doping is possible to change the layered structure of V₂O₅. The Li⁺ intercalation capacity and applicable current density of V₂O₅-TiO₂ nanorods electrodes are higher than pure V₂O₅ in case of molar ratio V/Ti = 75/25, but lower for molar ratio V/Ti = 50/50. Both morphology and poor crystalline structure affect the capacity.

ACKNOWLEDGEMENTS

Y.W. would like to acknowledge financial support from the Ford Motor Company Fellowship.

REFERENCES

- 1 M. Winter, J.O. Besenhard, M.E. Spahr, P. Novák: *Adv. Mater.* **10**, 725 (1998)
- 2 A. Shimizu, T. Tsumura, M. Inagaki: *Solid State Ionics* **63-65**, 479 (1993)
- 3 E. Portion, A. L.G.A. Salle, A. Verbaere, Y. Piffard, D. Guyomard: *Electrochim. Acta* **45**, 197 (1999)

- 4 P. Liu, S.-H. Lee, C.E. Tracy, J.A. Turner, J.R. Pitts, S.K. Deb: *Solid State Ionics* **165**, 223 (2003)
- 5 K. Takahashi, S.J. Limmer, Y. Wang, G.Z. Cao: *Appl. Phys. Lett.* **86**, 31 (2005)
- 6 G. Gu, M. Schmid, P.-W. Chin, A. Minett, J. Frayse, G.-T. Kim, S. Roth, M. Kozlov, E. Munoz, R.H. Baughman: *Nature Materials* **2**, 316 (2003)
- 7 J. Livage: *Chem. Mater.* **3**, 578 (1991)
- 8 D. O'Hare: In *Inorganic Materials*, D.W. Bruce, D. O'Hare (Eds.) (John Wiley & Sons, New York, 1991) p.165
- 9 B.E. Conway: *Electrochemical Supercapacitors* (Plenum, New York, 1999)
- 10 T. Watanabe, Y. Ikeda, T. Ono, M. Hibino, M. Hosoda, K. Sakai, T. Kudo: *Solid State Ionics* **151**, 313 (2002)
- 11 K. Takahashi, S.J. Limmer, Y. Wang, G.Z. Cao: *Jpn. J. Appl. Phys.* **44B**, 662 (2005)
- 12 K. Takahashi, S.J. Limmer, Y. Wang, G.Z. Cao: *J. Phys. Chem. B* **108**, 9795 (2004)
- 13 K. Takahashi, Y. Wang, G.Z. Cao: *J. Phys. Chem. B* **109**, 48 (2005)
- 14 V. Petkov, P.N. Trikalitis, E.S. Bozin, S.J.L. Billinge, T. Vogt, M.G. Kanatzidis: *J. Am. Chem. Soc.* **124**, 10157 (2002)
- 15 F. Artuso, F. Bonino, F. Decker, A. Lourenco, E. Masetti: *Electrochim. Acta* **47**, 2231 (2002)
- 16 F. Varsano, F. Decker, E. Masetti, F. Croce: *Electrochim. Acta* **46**, 2069 (2001)
- 17 B.B. Owens, S. Passerini, W.H. Smyrl: *Electrochim. Acta* **45**, 215 (1999)
- 18 N. Özer, S. Sabuncu, J. Cronin: *Thin Solid Films* **338**, 201 (1999)
- 19 K.H. Lee, G.Z. Cao: *J. Phys. Chem. B* **109**, 11880 (2005)
- 20 M.G. Minett, J.R. Owen: *J. Power Sources* **32**, 81 (1990)
- 21 C.J. Fontenot, J.W. Wiench, M. Pruski, G.L. Schrader: *J. Phys. Chem. B* **104**, 11622 (2000)
- 22 G.Z. Cao: *Nanostructures and Nanomaterials: Synthesis, Properties and Applications* (Imperial College Press, London, UK, 2004)
- 23 G.Z. Cao: *J. Phys. Chem. B* **108**, 19921 (2004)
- 24 T.L. Wen, J. Zhang, T.P. Chou, S.J. Limmer, G.Z. Cao: *J. Sol-Gel Science & Techn.* **33**, 193 (2005)
- 25 J.S. Reed: *Introduction to Principles of Ceramic Processing* (Wiley, New York, 1988)
- 26 F. Coustier, S. Passerini, W.H. Smyrl: *Solid State Ionics* **100**, 247 (1997)
- 27 A. Surca, S. Benèiè, B. Orel, B. Pihlar: *Electrochim. Acta* **44**, 3075 (1999)
- 28 B.B. Owens, W.H. Smyrl, J.J. Xu: *J. Power Sources* **81-82**, 150 (1999)